IRSTI 27.35.17 https://doi.org/10.26577/ijmph.2021.v12.i1.05

A.A. Issakhov, A.K. Manapova*

Kazakh-British technical university, Almaty, Kazakhstan
*e-mail: manapova.a.k.math@gmail.com

Numerical modeling of air flow inside the human nose cavity

Abstract. The complex structure of the human nasal cavity makes it difficult to study the flow of air in it, therefore, at present, mathematical and computer modeling is used for this purpose. These studies are relevant due to the development of inhalation methods for injections drugs into the nose, with the help of which surgery can be performed. Within the framework of the Navier-Stokes, temperature and concentration system of equations using the ANSYS Fluent application, a three-dimensional test calculation of the air flow in the human nasal cavity was carried out at various modes of inhalation, normal inhalation and during exercise. The laminar model was used to close the Navier-Stokes equations, and the SIMPLE method was used to perform the relationship between velocity and pressure. In the graphics package AutoCAD, a geometric three-dimensional model of the nasal cavity was built, reconstructed from images of the nose in coronary sections. As a result of numerical simulation, the fields of velocity, pressure, temperature and concentration were obtained. The obtained results were compared with the experimental data from [10] and the numerical results from [3]. The obtained results match with the experimental data. It was found that the inhaled air is heated and humidified to the state of the nasal tissue, the shells increase the rate of local transfer of heat and moisture by improving mixing and maintaining thin boundary layers, the capacity of a healthy nose exceeds the requirements necessary for conditioning the inhaled air under normal breathing conditions.

Key words: system of equations Navier-Stokes, anatomical model of the nose, coronary planes, flow structure, method SIMPLE, inhaled air conditioning.

Introduction

The nose is located at the beginning of the human respiratory tract and plays an important role in transporting air to the lungs, in purifying the air, in delivering drugs to the body during inhalation, etc. Physical deficiencies in the nasal cavity make it difficult to perform these functions. For treatment and surgery, in order to avoid unwanted complications, it is necessary to have a good knowledge of the structure of the nasal cavity and the structure of the movement of the inhaled gas.

Mathematical modeling of the air flow in the human nasal cavity can investigate the structure of the flow, which cannot be detected by modern instrumental methods, makes it possible to predict the results of real surgical operations, and can also help in determining the method of drug delivery during inhalation.

Studies of the flow of air in the human nasal cavity have been conducted since the 1990s, to which the works of the authors [1-6], etc. The first calculations were carried out only for one part of the nasal cavity, where the computational grid did not reach 100,000 cells [3, 4, 7]. In later works, one can see the results of the study of both sides of the nasal cavity, where the calculations were carried out for several 10 times larger numbers of grid cells.

The air flow in the human nasal cavity has been experimentally studied for decades in works [8-16].

In addition, the authors of [3, 17, 18-21] carried out an analysis of fluid dynamics (CFD) of the human nasal cavity, confirming the main experimental observations.

The first native publication on this topic appeared in 2016 [22], where a two-dimensional computational study of transport phenomena in model cross-sections of the nasal cavity of a normal human nose was investigated on the basis of a two-dimensional incompressible system of Navier-Stokes equations. In the mentioned work, the methods of finite volumes and projection are applied. Research has shown that a normal nose can maintain balance even under extreme conditions.

In [23], studies of airflow transfer in a nasal cavity model for normal inspiratory rate in various

© 2021 al-Farabi Kazakh National University

environmental conditions were carried out, where numerical results showed that during normal breathing, the human nose copes with the metabolism of heat and relative humidity in order to balance the alveolar conditions within.

In [24], numerical methods based on an anatomically accurate model of the nose were tested. It was found that the laminar model achieves good similarity with experimental results under calm breathing conditions (180 ml / s) and performs better than the turbulent RANS model. The turbulent RANS models gave more accurate predictions for the increase in respiration rate, but the LES and DNS results were better. As expected, the LES and DNS can provide accurate forecasts of nasal airflow in all conditions, but their computational costs are 100 times greater. Among all the tested RANS models, the standard model most closely matches the experimental values in terms of the velocity profile and turbulence intensity.

For more efficient computation of numerical simulation of air transport in the human nasal cavity, parallel computing technologies are used. In [25], a two-dimensional numerical simulation of air transport in model sections of the nasal cavity by the projection method was carried out, where the algorithm is parallelized using geometric decompositions. As a result, the effectiveness of various methods of decomposition of the computational domain was determined.

Mathematical model

Mathematical model is

$$\begin{cases} \nabla \cdot U = 0 \\ \dfrac{\partial U}{\partial t} + (U \cdot \nabla) U = -\dfrac{1}{\rho} \nabla P + \nu \nabla^2 U \\ \dfrac{\partial T}{\partial t} + (U \cdot \nabla) T = \dfrac{k}{\rho c_p} \nabla^2 T \\ \dfrac{\partial C}{\partial t} + (U \cdot \nabla) C = -D \nabla^2 C \end{cases} \quad (1)$$

where U – velocity vector, T – temperature, C – concentration, t – time, x, y, z – spatial coordinates, ρ – density, k – thermal diffusivity, c_p – specific heat, ν – kinematic viscosity, D – molecular diffusion coefficient, ∇^2 – Laplacian operator.

Initial conditions: $u_{t=0} = v_{t=0} = w_{t=0} = 0$, $T_{t=0} = 32^0$C, $C_{t=0} = 0{,}0235\ kgH_2O/m^3$.

Input boundary conditions for speed: for normal breathing $u = v = w = 1$ *м/с* and for breathing during the exercise $u = v = w = 2.5$ *м/с*.

Boundary conditions on the inlet for temperature and concentration: $T_{t=0} = 25^0$C, $C_{t=0} = 0{,}0047\ kgH_2O/m^3$.

The boundary conditions for the velocity at the walls of the nasal cavity and turbinate are specified as no slip conditions.

Boundary conditions on the walls for temperature and concentration: $T_{wall} = 37^0$C, $C_{wall} = 0{,}0438\ kgH_2O/m^3$.

The ANSYS FLUENT application package is used for numerical modelling. The laminar model was used to close equations (1), and the SIMPLE algorithm was used to relate pressure and velocity.

56 forms of the transverse coronary planes of the nasal cavity obtained from [26] and were digitized, restored in the graphic program Autocad. Final result was constructed as a geometric model of the nasal cavity of a real person (Figure 1).

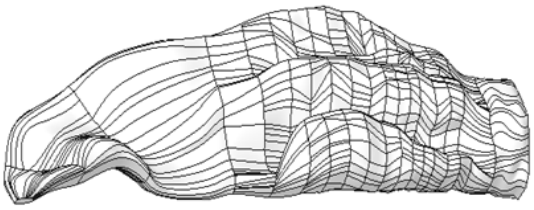

Figure 1 – Constructed 3D model of the nasal cavity

The right side of the nasal cavity was used during calculation, in which the *Y* axis is directed vertically upward, the *X* axis is directed from the entrance to the nasopharynx along the main direction of flow. Computational grid consists of 692 158 elements.

Computational fluid dynamics (CFD) analysis of nasal function is studied with the article [3]. The numerical results were compared with the detailed experimentally measured velocity profiles from [10] and the numerical results from [3].

The results were obtained in the indicated lines of 4^{th}, 6^{th}, 8^{th}, 9^{th} planes (Figure 2).

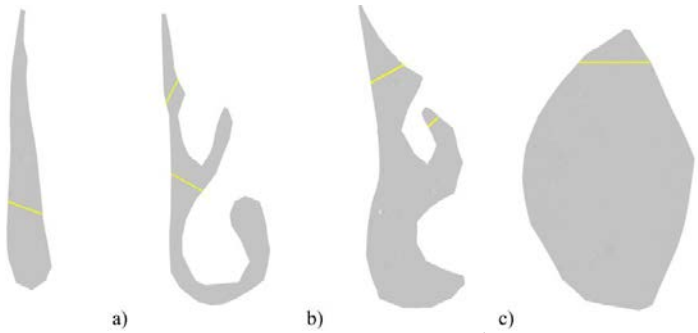

Figure 2 – a – a line with a dimension of 2.66 mm in 4th plane; b – lines with dimensions 1.42 mm and 1.81 mm in 6th plane; c – lines with dimensions 2.26 mm and 2.29 mm 8th plane; d) line with a size of 3.28 mm in 9th plane

Numerical results

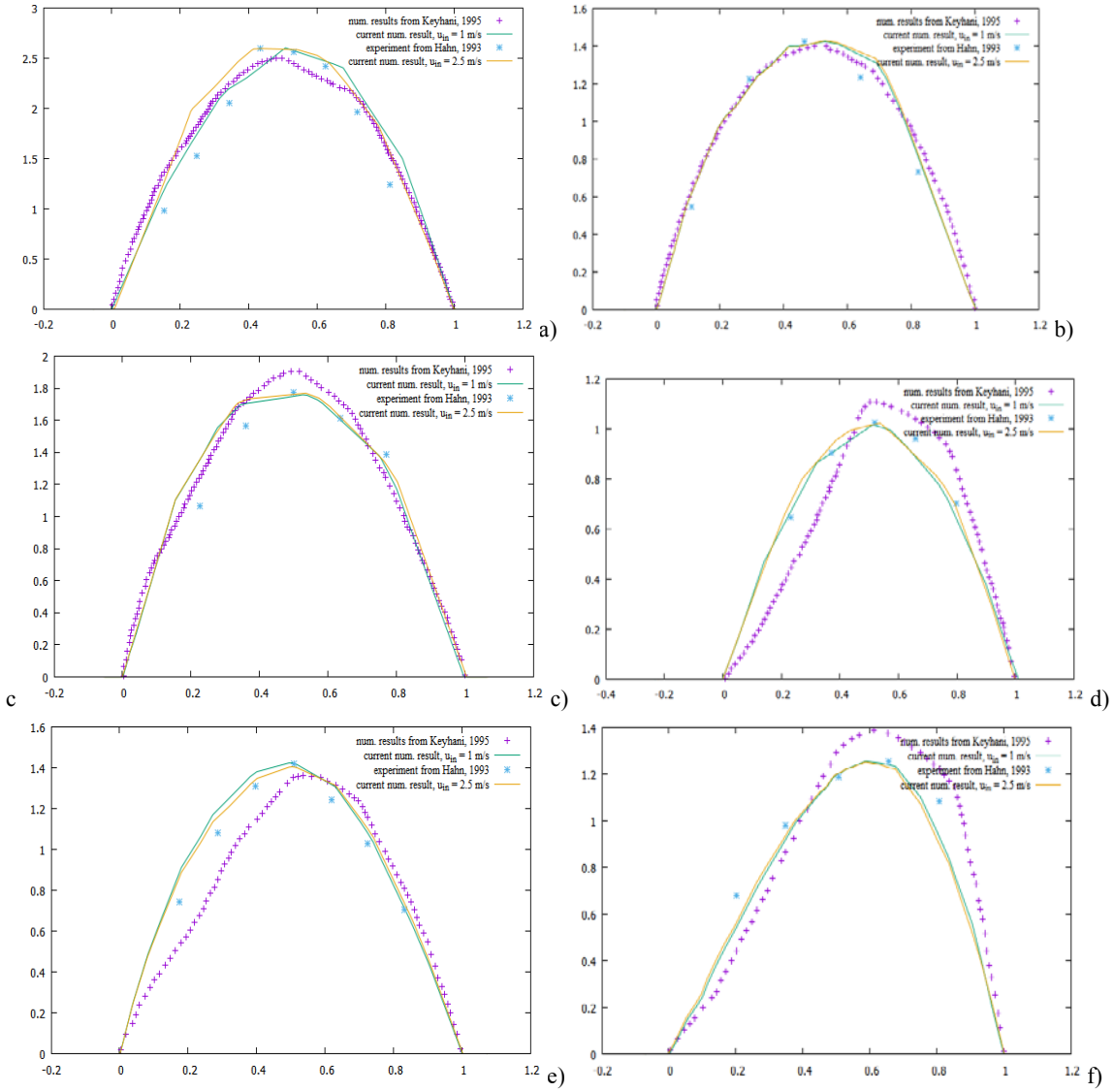

Figure 3 – a) Velocity profiles U in 4th plane in line 2.66; b) Velocity profiles U in 6th plane in line 1.42; c) Velocity profiles U in 6th plane in line 1.81; d) Velocity profiles U in 8th plane in line 2.26; e) Velocity profiles U in 8th plane in line 2.29; f) Velocity profiles U in 9th plane in line 3.28

The results of the current numerical simulation are in good agreement with the experimental data from [10], as shown in Figures 3 (a-f). The profiles were dimensioned for maximum speed. Dimensionless distance was from the lateral to the medial sides of the airways.

Numerical results match with experimental measurements less than 20 percent at the most comparison locations. More accurate agreement was obtained at many points in the model. The difference between the results can be attributed to different sources of numerical and experimental errors.

In figure 4 velocity contours show the appearance of vortices in the vicinity of the turbinate itself.

In figure 5 due to air heating, the temperature increases by 37°C.

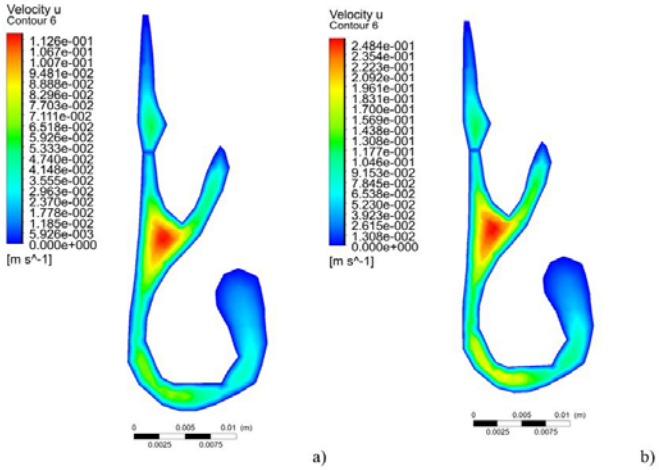

Figure 4 – Velocity contours in cross-section 6 with inlet velocities a – 1 m/s and b – 2,5 m/s

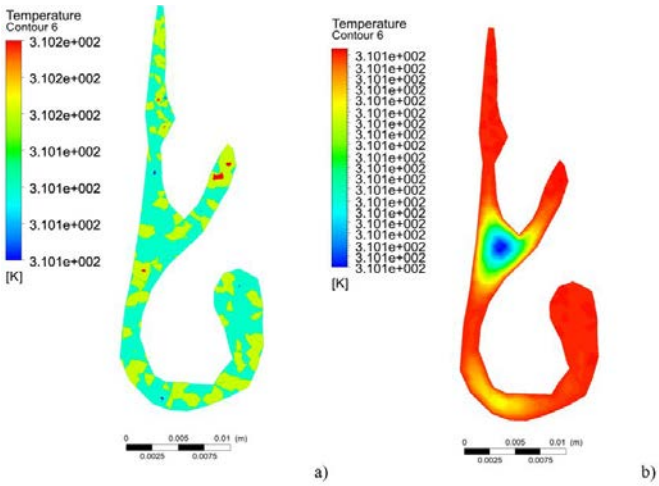

Figure 5 – Temperature contours in cross-section 6 with inlet velocities a – 1 m/s and b – 2,5 m/s

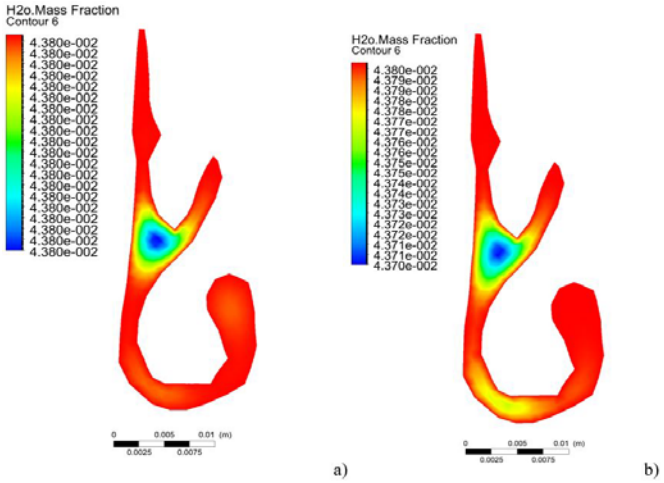

Figure 6 – Concentration contours in cross-section 6 with inlet velocities a – 1 m/s and b – 2,5 m/s

In the vicinity of the shell, moisture increases due to the narrowing of the nasal cavity. In figure 6 moisture concentration reaches 0.438 kgH_2O/m^3.

Conclusion

A three-dimensional numerical simulation of the nasal cavity models has been carried out due to lack of studying problems of air transport phenomena in it. Inhaled air is heated and humidified to the state of the nasal tissue. The shells increase the rate of local heat and moisture transfer by improving mixing and maintaining thin boundary layers. During an average inhalation (when the speed is maximum), a rapidly moving air core dominates in the flow of inhaled air, and as a result, the instantaneous heat and mass exchange of the inhaled air is significantly reduced.

The nose can handle a range of extreme conditions. However, impaired circulation or surface moisture can reduce the rate of heat or moisture flows into the inhaled air. The capacity of a healthy nose exceeds the capacity required for conditioning the inhaled air under normal breathing conditions. As a consequence, it can be effective during heavy breathing and variety of entry conditions, including a scrubbing process to remove toxic gases and particles.

In future studies, it will be necessary to improve the detailed description of the processes' dynamics of heat transfer, water and soluble gas on the surface of the mucous membrane, especially in the region of the turbinate.

References

1 Garcia G.J., Bailie N.A., Martins D.A., Kimbell J.S. "Atrophic rhinitis: A CFD study of air conditioning in the nasal cavity." *Journal of Applied Physiology*. 103 (2007): 1082–1092.

2 Hörschler I., Schröder W., Meinke M. "Numerical analysis of the impact of the nose geometry on the flow structure. Part II: Nasal valve and lower turbinate." *Computational Fluid Dynamics Journal.* 16 (2008): 243–260.

3 Keyhani K., Scherer P.W., Mozell M.M. "Numerical simulation of airflow in the human nasal cavity." *J. Biomech. Engng.* 117 (1995): 429–441.

4 Lindemann J., Keck T., Wiesmiller K., Sander B., Brambs H.J., Rettinger G., Pless D. "A numerical simulation of intranasal air temperature during inspiration." *The Laringoscope.* 114 (2004): 1037–1041.

5 Rhee J.S., Cannon D.E., Frank D.O., Kimbell J.S. "Role of virtual surgery in preoperative planning. assessing the individual components of functional nasal airway surgery." *Arch. Facial. Plast. Surg.* 14 (2012): 354–359.

6 Segal R.A., Kepler G.M., Kimbell J.S. "Effect of differences in nasal anatomy on airflow distribution: a comparison of four individuals at rest." *Annals of Biomedical Engineering.* 36 (2008): 1870–1882.

7 Wen J., Inthavong K., Tian Z.F., Tu J.J., Xue C.L., Li C.G. "Airflow pattern in both sides of a realistic human nasal cavity for laminar and

turbulent conditions." *Proceedings of 16th Australasian Fluid Mechanics Conference*. Gold Coast, (2009): 68–74.

8 Churchill S.E., Shackelford L.L., Georgi J.N, Black M.T. "Morphological variation and airflow dynamics in the human nose." *American Journal of Human Biology.* 16 (2004): 625–638.

9 Girardin M., Bilgen E., Arbour P. "Experimental study of velocity fields in a human nasal fossa by laser anemometry." *Annals of Otology, Rhinology and Laryngology.* 92 (1983): 231–236.

10 Hahn I., Schere P.W., Mozell M.M. (1993). "Velocity profiles measured for airflow through a large-scale model of the human nasal cavity." *Journal of Applied Physiology.* 75 (1993): 2273–2287.

11 Hornung D.E., Leopold D.A., Youngentob S.L., Sheehe P.R., Gagne G.M., Thomas F.D. "Airflow patterns in a human nasal model." *Archives of Otolaryngology—Head and Neck Surgery.* 113 (1987): 169–172.

12 Kelly J.T., Prasad A.K., Wexler A.S. "Detail flow patterns in the nasal cavity." *Journal of Applied Physiology.* 89 (2000): 323–337.

13 Kim S.K., Chung S.K. (2004). "An investigation on airflow in disordered nasal cavity and its corrected models by tomographic PIV." *Measurement Science and Technology.* 14 (2004): 1090–1096.

14 Park K.I., Brucker C., Limberg W. "Experimental study of velocity fields in a model of human nasal cavity by DPIV." *In B. Ruck, A. Leder, & D. Dopheide, Laser anemometry advances and applications: Proceedings of the seventh international conference, University of Karlsruhe, Karlsruhe, Germany.* (1997).

15 Schreck S., Sullivan K.J., Ho C.M., Chang H. K. "Correlations between flow resistance and geometry in a model of the human nose." *Journal of Applied Physiology.* 75 (1993): 1767–1775.

16 Swift D.L., Proctor D.F. "Access of air to the respiratory tract." *In J. D. Brain, D. F. Proctor, L. M. Reid, Respiratory defense mechanisms: Part I.* (1977): 63–93.

17 Subramaniam R.P., Richardson R.B., Morgan K.T., Kimbell J.S. "Computational fluid dynamics simulations of inspiratory airflow in the human nose and nasopharynx." *Inhalation Toxicology.* 10 (1998): 91–120.

18 Horchler I., Meinke M., Schröder W. "Numerical simulation of the flow field in a model of the nasal cavity." *Computers and Fluids.* 32 (2003): 39–45.

19 Weinhold I., Mlynski G. "Numerical simulation of airflow in the human nose." *European Archives of Otorhinolaryngology.* 261 (2004): 452–455.

20 Shi H., Kleinstreuer C., Zhanga Zh. "Modeling of inertial particle transport and deposition in human nasal cavities with wall roughness." *Aerosol Science.* 38 (2007): 398 – 419.

21 Kleinstreuer C., Zhang Z. (2003). "Laminar-to-turbulent fluid-particle flows in a human airway model." *International Journal of Multiphase Flow.* 29 (2003): 271–289.

22 Issakhov A., Yessenkozha A.M. "Mathematical modelling of air flow in the human respiratory system." *International Journal of Mathematics and Physics*. 27 (2016): 27-32.

23 Issakhov A., Zhandaulet Y., Abylkassymova A., Issakhov A. "A numerical simulation of air flow in the human respiratory system for various environmental conditions." *Theoretical Biology and Medical Modelling.* 18 (2021).

24 Li Ch., Jiang J., Dong H., Zhao K. "Computational modeling and validation of human nasal airflow under various breathing conditions." *Journal of Biomechanics*. http://dx.doi.org/10.1016/j.jbiomech.2017.08.031

25 Issakhov A., Abylkassymova A. "Application of parallel computing technologies for numerical simulation of air transport in the human nasal cavity." *Springer international publishing, Innovative computing, optimization and its application.* (2018).

26 Liu Y., Johnson M. R., Matida E. A., Kherani S., and Marsan J. "Creation of a standardized geometry of the human nasal cavity" *J Appl Physiol.* 106 (2009): 784–795.